JOURNAL OF THERMOPHYSICS AND HEAT TRANSFER
Vol. 7, No. 4, Oct.–Dec. 1993

In Situ Plume Radiance Measurements from the Bow Shock Ultraviolet 2 Rocket Flight

Peter W. Erdman* and Edward C. Zipf†
University of Pittsburgh, Pittsburgh, Pennsylvania 15260
Patrick Espy‡ and Carl Howlett§
Utah State University, Logan, Utah 84322
Carol Christou¶ and Deborah A. Levin¶
Institute for Defense Analyses, Alexandria, Virginia 22311
Robert J. Collins**
University of Minnesota, Minneapolis, Minnesota 55455
and
Graham V. Candler††
North Carolina State University, Raleigh, North Carolina 27695

The ultraviolet spectrum (200–400 nm) of the plumes generated by the second- and third-stage engines of a Strypi XI rocket and of the Mach 17 re-entry bow shock were obtained by a sounding rocket experiment launched from the Barking Sands Research Range (Kauai, Hawaii) on February 18, 1991, at 14:30 GMT. The re-entry optical data were obtained as the payload descended from 120 to 65 km with a vehicle velocity of 5.1 km/s. The intensities of the vacuum ultraviolet resonance radiation emitted by atomic oxygen and hydrogen in the bow shock at 130.4 and 121.5 nm, respectively, were also measured. Complementary Langmuir probe measurements provided data on the total plasma density and electron temperature in the boundary layer.

Introduction

THE bow shock ultraviolet rocket experiment 2 was the second in a series of flight experiments[1,2] designed to measure radiation produced by hypersonic vehicles. This article deals primarily with the design of the UV diagnostics experiment (UVDE) payload and with the optical data obtained from the second- and third-stage motor plume measurements during the Strypi XI flight. The UVDE was launched on February 18, 1991 at 14:30 GMT from the Barking Sands Research Range on Kauai, Hawaii. Figure 1 shows the rocket velocity and altitude as well as staging and hardware deployment events for the entire mission. The Castor I booster lifted the payload to an altitude of 120 km. An attitude control system was then used to orient the payload nearly horizontal during the Antares II second-stage and Star-27 third-stage engine burns which accelerated the payload to the re-entry velocity of 5.1 km/s. Figure 2 shows the rocket velocity and altitude as a function of time after launch (TALO) during the Antares and Star motor burns, the portion of the trajectory for which data will be presented here. Note that the altitude variation during these stages is small; but the velocity increases substantially during the last stage. The re-entry data from this flight will be presented at a later date.

Payload Instrument Description

The instrumentation on the payload included a forward-viewing section consisting of a rapid scan spectrometer, eight quartz fiber optic photometers, an electron density microprobe, and two vacuum ultraviolet (VUV) photometers. The plume observations were performed with an aft-observing instrumentation section that consisted of a scanning spectrometer and eight photometers. These instruments viewed the Antares and Star-27 plumes through three periscopes that were erected after the Castor motor burnout and nose cone ejection. The periscopes were ultimately jettisoned a few seconds after the third-stage Star-27 motor burnout, and the aft instrumentation then observed radially to the payload axis during re-entry. Numerous temperature monitors also provided support information for total re-entry heating. Figure 3 shows the arrangement of the instrumentation in the payload.

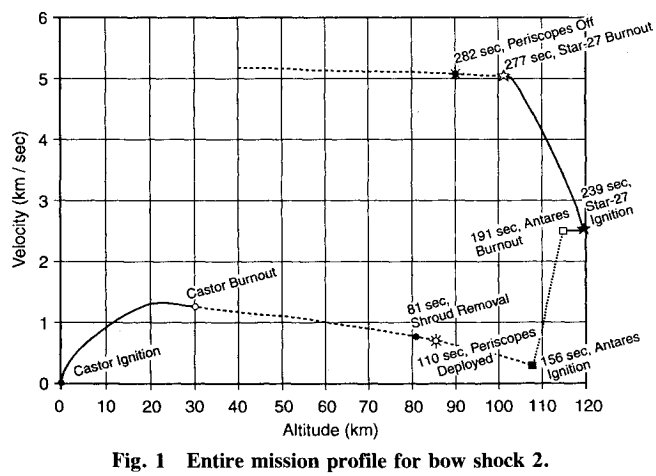

Fig. 1 Entire mission profile for bow shock 2.

Presented as Paper 92-0124 at the AIAA 30th Aerospace Sciences Meeting and Exhibit, Reno, NV, Jan. 6–9, 1992; received Sept. 23, 1992; revision received Jan. 28, 1993; accepted for publication Jan. 29, 1993.

*Research Associate Professor, Department of Physics and Astronomy. Member AIAA.
†Professor, Department of Physics and Astronomy. Member AIAA.
‡Research Associate Professor, Department of Physics.
§Technical Program Manager, Center for Space Engineering. Member AIAA.
¶Research Staff Member, Science and Technology Division. Member AIAA.
**Professor, Department of Electrical Engineering.
††Assistant Professor, Department of Mechanical and Aerospace Engineering. Member AIAA.

The rapid scanning spectrometers covered the 190–400-nm wavelength range in a 1.0-s scan. These instruments were a modified Fastie-Ebert design of 150-mm focal length, with a 10-deg (total angle) field of view (FOV) for the forward-viewing instrument and a 2 × 8-deg FOV for the aft plume spectrometer. Each spectrometer was fitted with two exit slits—each with its own photomultiplier detector. Equal width, curved slits were selected to give 1-nm resolution (at 400 nm) as a reasonable compromise between throughput and resolution. Optics were all Al-MgF_2 overcoated Zerodur, superpolished for reduced scattering. The grating was from a new 1800-g/mm classically ruled master made by Hyperfine, Inc. This was a very low noise, highly efficient grating that considerably enhanced the effectiveness of this instrument. Each photomultiplier detector had completely separate high-voltage supplies and data systems, each with its own pulse counting system which also operated in parallel with an electrometer channel. This analog channel was designed to handle very high signal levels when counting rates would be well beyond those which could be accommodated by a pulse counting system alone. This was required during both the plume measurements and the late part of the re-entry period. The analog signals were digitized by fast 16-bit A/D converters before transmission by the telemetry system. The high-speed stepper motor wavelength drive system made a 0.2-nm wavelength step every 1.28 ms, in synchronization with the data system. This short integration time demanded very high instrument throughput in order to yield a statistically significant number of counts per channel—which become shot noise limited even at very high counting rates.

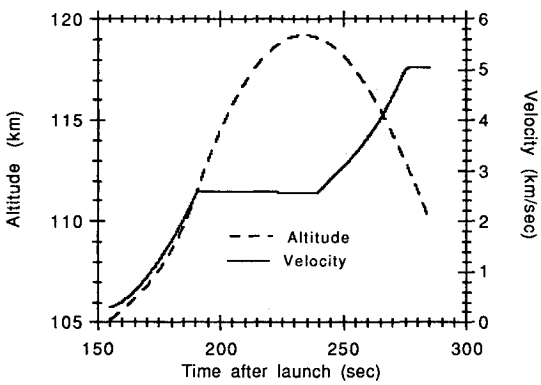

Fig. 2 Rocket velocity and altitude during Antares and Star motor burns. Note that the rocket altitude is essentially constant.

Design considerations required 1) that the spectrometer have high intrinsic dynamic range (10 orders of magnitude from maximum tolerable signal to a signal/dark count noise ratio of unity); 2) that it acquire individual spectra rapidly, and 3) that the instrument have very low scattered light levels. The design requirements were dictated by the model predictions of large variation in signal intensity with wavelength for the plume measurements and that the signal levels on re-entry would increase to very high levels, hence, good altitude resolution and total dynamic range were important for a successful measurement. The relatively long motor burn times (30 s) and the shallow re-entry angle only required a modest scan speed of 1 s/scan to give sufficient temporal and spatial resolution. In the previous bow shock 1 flight,[1] the instrument scanned at four times this rate.

The spectral range between the short wavelength cutoff of quartz at 190 and 400 nm was covered by two separate detectors with different photocathodes, one CsTe and the other Bialkali. The Bialkali detector was blocked to radiation beyond 420 nm and wavelengths shorter than 240 nm by a Schott black glass filter. This strategy reduced any concern about a longer wavelength source of scattered light and it eliminated any second-order contamination from strong short wavelength radiation. One detector nominally covered the first hundred nanometers of the scan and the second detector covered the remainder. However, these detectors and their exit slit spacings were chosen to provide ~50-nm overlap in wavelength coverage for redundancy in case of the failure of one detector,

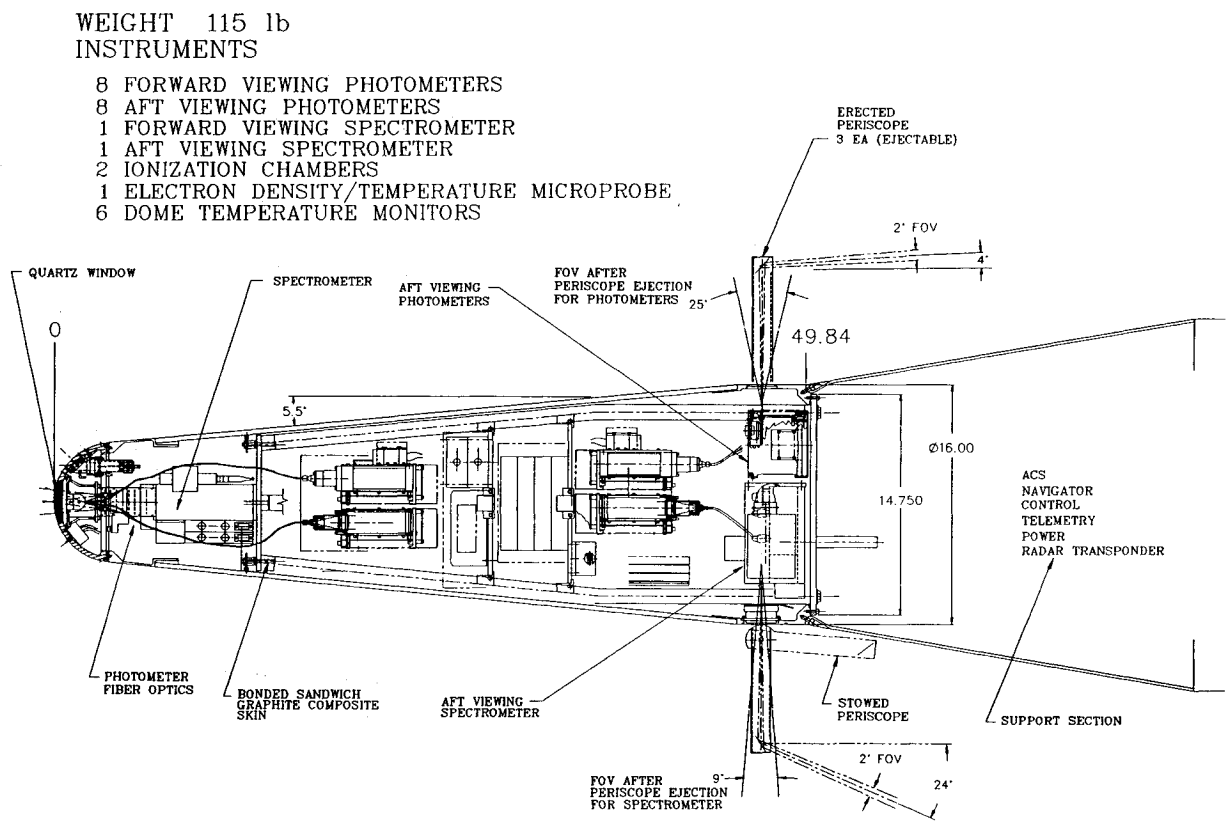

Fig. 3 Simplified schematic diagram showing the location of the optical instrumentation and microprobe on the UVDE payload.

and as a check on the independent calibrations of each channel and its data system. Excellent agreement between the two detectors was found in the reduced data, confirming that each performed nominally.

The forward-viewing spectrometer was used to measure the bow shock ultraviolet radiance—primarily from the nitric oxide gamma band system. The aft spectrometer was to view the rocket motor plumes until the end of the Star-27 burn when the periscopes were ejected. It then viewed in the direction perpendicular to the vehicle's longitudinal axis.

The instrument package also included 16-UV filtered photometers. These were located on inner decks in the payload, and were coupled to the forward and aft windows with quartz fiber optics. At the exit of this fiber, a lens focused on the small diameter fiber formed a parallel beam incident on an interference filter and then onto the photomultiplier. The photocathodes were selected according to the spectral feature of interest.

The photometers were designed in two groups of eight: one group dedicated to viewing forward and the other aft through the periscopes. These photometer groups were constructed as two banks of four detectors, each with its own high-voltage supply. The individual detectors also had both an analog electrometer channel and a digital pulse counting channel in order to increase the total dynamic range to approximately eight orders of magnitude. The analog channels were digitized with a 16-bit A/D converter before transmission over the telemetry system with a sample rate of 548 samples/s. The total angle of the entrance FOV of each forward photometer was ~25 deg, and the aft-viewing photometers had the same 2 × 8-deg FOV as the aft spectrometer.

Design considerations required that the forward-viewing photometers achieve the highest temporal resolution possible within the constraints of instrument size, sensitivity, and data rate. Along with the measurement of the motor plumes' radiance and the bow shock ultraviolet radiance as a function of altitude and velocity, the variations in intensity with position from the stagnation point were also measured by this system of separate photometers with viewing angles of 0, 30, and 50 deg from the vehicle centerline. Re-entry data obtained from the instruments will be presented at a later time. For completeness, Table 1 shows the molecular spectral feature and wavelength characteristics associated with these instruments.

The spectral characteristics and the payload location of each of the aft-viewing photometers is shown in Table 2. One group of four aft-viewing photometers observed at an angle of 4 deg to the vehicle axis, the same as the aft spectrometer. These are also referred to as the "intrinsic core" photometers. The other four aft-viewing photometers observed at an angle of 25 deg to the vehicle axis (outside the intrinsic core of the plume). These are designated as the "far-field" photometers. The two aft-viewing geometries were chosen to study two different regions of the plume: e.g., the 4-deg geometry viewed a spatial region known to contain molten alumina particulates vs a spatial region that is less influenced by the particulates (i.e., 25 deg). The companion theory article discusses these spatial regions in detail.[3] The 230-nm photometers were configured to obtain the highest signal sensitivity.

Table 1 Forward-viewing photometers

Spectral feature	Center wavelength, nm	Filter width, nm	Location, deg
NO	215	6	0
NO	230	51	0, 30, 50
N_2^+	391.4	2.5	0
OH	309	8	0, 30, 50

Table 2 Aft plume-viewing photometer characteristics

Center wavelength, nm	Filter width, nm	Minimum signal, W/cm² μmsr
Intrinsic core viewing (4 deg)		
230	51	1.0×10^{-10}
309	8	1.1×10^{-7}
422	10	2.7×10^{-8}
Far-field viewing (25 deg)		
230	51	7.3×10^{-11}
309	8	7.0×10^{-8}
391	25	7.8×10^{-8}
422	10	3.6×10^{-8}
471	10	1.5×10^{-8}

Absolute calibrations for both the spectrometer and the photometer channels were performed with a deuterium arc lamp. This UV continuum source was calibrated for irradiance with National Bureau of Standards traceable standards. A white diffuse reflectance screen of Halon, large enough to fill the FOV of the respective instrument being calibrated, was illuminated by the lamp and then observed with the instrument. Cross calibrations between the spectrometers and photometers were also performed in the field just before launch under identical conditions in order to minimize the systematic errors. Separate transmission calibrations of the quartz viewing windows in the dome were performed on the actual flight windows. Finally, a calibration was performed with the fully assembled payload through the flight data systems and the telemetry system as an end to end system check. No vacuum system was employed, therefore, it was not possible to properly calibrate the spectrometer data acquired below 200 nm.

Several spectral line sources with known, identifiable, wavelength standards were used to properly locate the spectrometer wavelength scan and establish the wavelength interval. The bandpass of each interference filter used in the photometers was verified by laboratory measurements with a scanning spectrometer and continuum light sources.

The entire payload was hermetically sealed and remained pressurized during the flight. Before launch, the payload was vigorously purged and then positively pressurized with dry Argon. This gas then continued to flow out the small viewing ports used for the VUV measurements, thereby reducing the absorption of that radiation as well as insuring the stability of the calibration of the other instruments by eliminating water vapor or particulate contamination of the optics inside the payload.

As a result of these calibration efforts, the absolute accuracy of the visible and UV optical measurements is generally within 20%. However, for the spectrometers the calibration accuracy at wavelengths between 210 and 200 nm decreases to approximately 30% due to the uncertainty in the relative atmospheric absorption during the course of the calibration and in flight. Also, beginning at the wavelength of ~390 nm, the accuracy of the spectrometer calibration steadily degrades to approximately 50% at 400 nm in the analog mode of operation. This is a result of the decreasing sensitivity of the instrument and the decreasing flux of the deuterium calibration lamp at the longest wavelengths—the combination of which makes the calibration excessively sensitive to the A/D converter offset. The digital mode is unaffected by this problem, but the high fluxes observed in the plume measurements required the use of the analog mode at the longest wavelengths.

Data

Figure 4 shows the data obtained from the 230-, 309-, and 422-nm photometers observing the "near field" intrinsic core of the motor plumes (~4 deg from the vehicle axis). The signal decay observed in the 230-nm photometer after the Antares motor shutoff (which is above the sensitivity limit of the instrument) was not initially understood. Similar behavior was observed after Star-27 motor burnout as well. The signal decays to the stellar background limit which has been measured to be about 7.8×10^{-10} W/cm² μsr.[4]

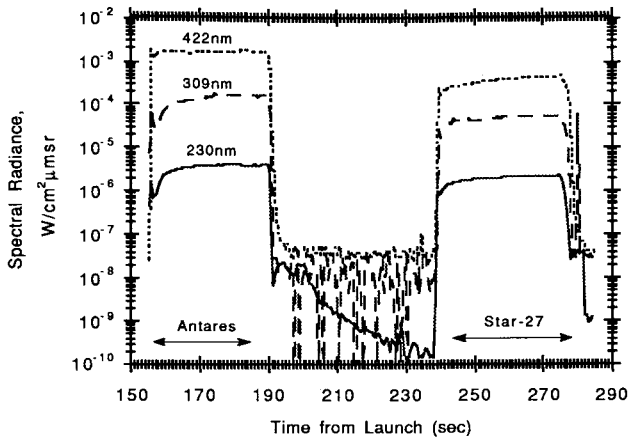

Fig. 4 Radiance as a function of TALO from intrinsic core-viewing photometers. Data is averaged over a time interval of 0.5 s. Center wavelength is indicated above the respective curves.

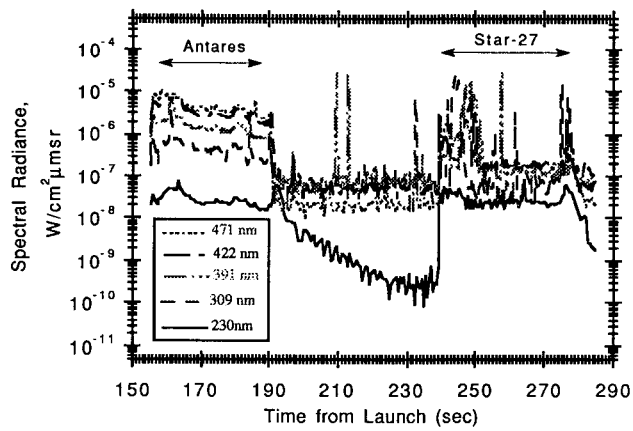

Fig. 5 Radiance as a function of TALO from far-field-viewing photometers. Data is averaged over a time interval of 0.5 s.

Figure 5 shows similar data obtained from the 5 far-field (~25 deg from the vehicle axis) photometers. In both Figs. 4 and 5 the data has been averaged over 0.5 s. Signal levels are seen to be lower than those observed from the intrinsic core (Fig. 4).

Figures 6 and 7 show the plume spectra obtained from the aft-viewing spectrometer during the Antares II (TALO of 172 s) and Star-27 (TALO of 257 s) motor burns. Each of these is a single scan of the spectrometer. These flight data show that the UV emission from both motor plumes were nearly continuous in character. The Planck blackbody formula almost accounts for the spectral distribution assuming the alumina particle phase transition temperature of 2320 K. The scaling factors reflect the particle density along the 4-deg FOV of the spectrometer. The deviation from the scaled blackbody curves at wavelengths greater than 300 nm is due to the optical properties of the Al_2O_3 particles. In the companion article[3] the spectra are analyzed in greater detail. The spikes at the short wavelength end of the spectrum are due to shot noise at these low signal levels that can be reduced ultimately by coherently summing several adjacent spectra (dozens of scans were made of each motor burn). The notch that is clearly present in Figs. 6 and 7 near 261 nm is due to absorption by cool AlCl in the plume gas.[5]

Figure 8 shows a comparison of the signal observed in the 4- and 25-deg 230-nm photometers as a function of TALO. During the motor burns the difference in signal between the two viewing angles is seen to be about two and a half orders of magnitude. However, after engine shutoff (e.g., TALO of 190–230 s), the signal levels are much closer in both the 4- and 25-deg viewing photometers. This comparison suggests that the spectral content of the measurements taken after engine shutoff are different than those obtained during the steady-state burns. The 230-nm photometers give a detailed time history of the radiation; but, have poor spectral resolution.

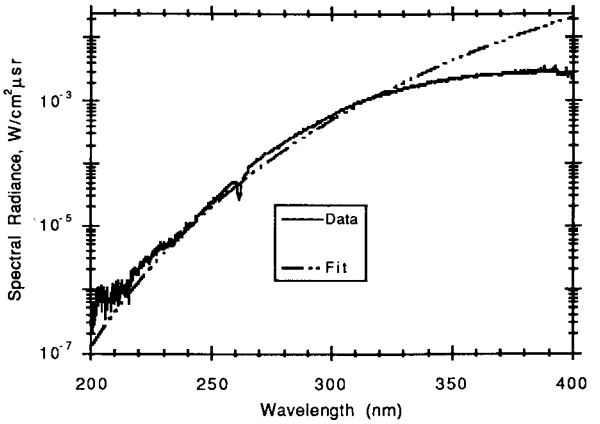

Fig. 6 Ultraviolet spectrum of the Antares plume and a 2320 K blackbody fit to the data at a temperature of 2320 K scaled by a factor of 10. Start of scan at 172-s TALO.

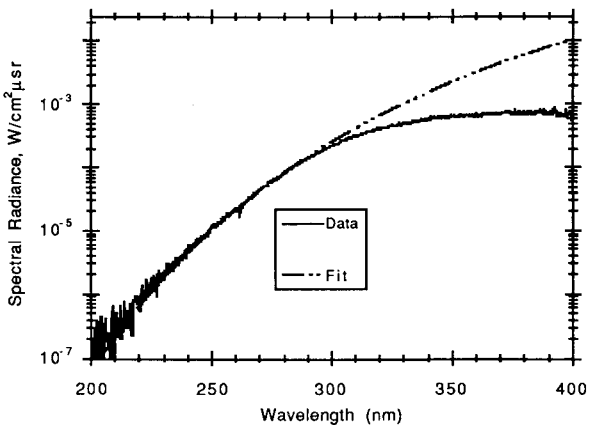

Fig. 7 Ultraviolet spectrum of the Star-27 plume and a 2320 K blackbody fit to the data at a temperature of 2320 K scaled by a factor of 20. Start of scan at 257-s TALO.

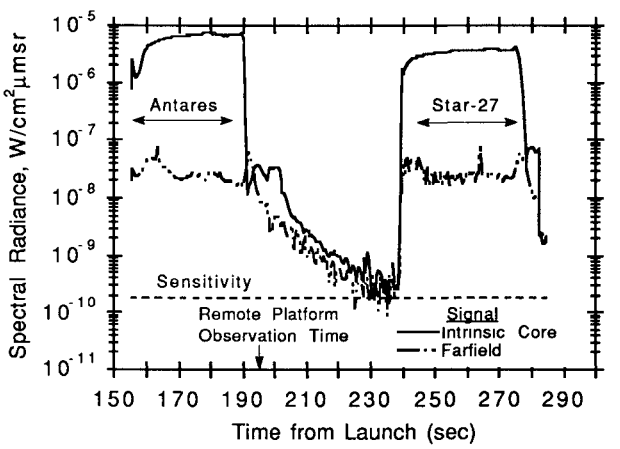

Fig. 8 Comparison of intrinsic core (4 deg) and far-field (25 deg) radiance from the 230-nm photometers.

Figure 9 shows a spectrum taken after Antares motor shutoff. In contrast with Figs. 6 and 7, this spectrum does not show continuum particulate gray body emission. The molecular emission that is observed is due to the CO Cameron band transition, a spin forbidden transition from the $a^3\Pi$ to the

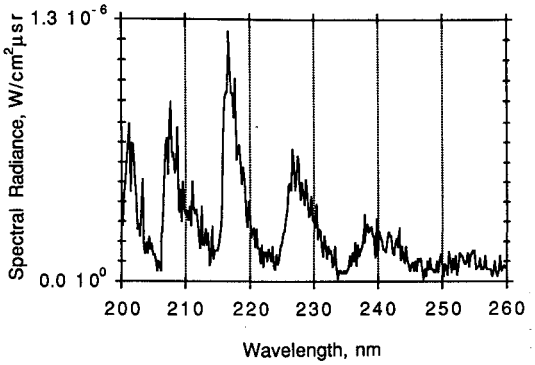

Fig. 9 Cameron band spectra measured approximately 4 s after Antares engine shutoff.

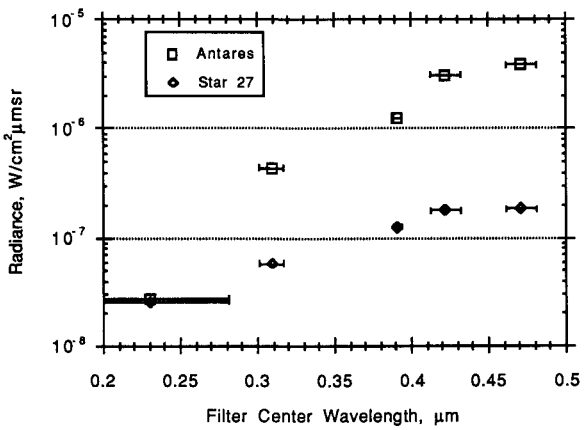

Fig. 10 Far-field radiance values as a function of photometer filter center wavelength at TALO of 174 s for the Antares and 255 s for the Star-27 data. Horizontal bars show filter half-width wavelengths.

$X^1\Sigma^+$ state. Justification for this assignment and theoretical interpretation of this data will be presented in the accompanying article.[3] This data represents the first in-flight verification of molecular emission in solid-propellant rocket motors.

The identification of molecular emission under conditions where the radiation is not dominated by the particulates suggests that molecular emission may also be present during the steady-state burns in both the 4- and 25-deg photometers. Due to inadequate preflight predictive capabilities of the signal levels that could be expected in the far field, a spectrometer was not dedicated to that region. The far-field photometers, centered at five distinct wavelengths, provide some indication of the spectral behavior of that emission. Figure 10 shows a summary of photometer radiances taken during the steady state Antares and Star-27 motor burns. The spectral dependence of the two curves was found to be different than the 2320 K gray body fit obtained for the data shown in Figs. 6 and 7. These data imply a significantly higher temperature than could be attributed to particulate emission. However, spectroscopic data on any future flights is required to unambiguously understand the far-field plume regime.

Conclusions

All the payload instrumentation in both the forward- and aft-viewing sections performed nominally throughout flight. Spectra obtained during the motor burns show evidence of gray body particulate emission and molecular absorption features that have also been observed in ground-based chamber measurements.[5] Comparison with spectrometer and far-field photometer data provided insight into the signal observed after engine shutoff. The first identification of CO Cameron band emission in a solid rocket motor propellant was obtained. The companion article[3] discusses our understanding of these observations at a fundamental level.

Acknowledgments

UVDE was developed by the Innovative Science and Technology Office of the Strategic Defense Initiative Organization in order to validate aerodynamic and radiative transfer models applicable to re-entry conditions and to measure the intensity and spectral distribution of the ultraviolet radiation emitted by the Antares and Star-27 engine plumes. The design, construction, and calibration of the payload instrumentation involved a collaborative effort among many institutions. Utah State University served as overall program manager for this instrument package and built the photometers and atomic oxygen and hydrogen resonance radiation detectors. The University of Pittsburgh provided the two rapid scanning UV spectrometers and the electron probe module. The Sandia Corporation was responsible for the telemetry, payload, and vehicle integration and provided launch support. The Institute for Defense Analyses was responsible for the optical radiation level predictions and interpretation of theory, while North Carolina State University provided assistance with the flowfield and radiation modeling as well as computer support. Fundamental aspects of the models have also been investigated by other groups under a related program managed by the Army Research Office. In addition, ground-based and satellite remote observations of the rocket plumes were made from the AMOS optical site and by the LACE/UVPI satellite. Results obtained from these platforms are presented elsewhere.

References

[1]Erdman, P. W., Zipf, E. C., Espy, P. J., Howlett, C. L., Levin, D. A., Loda, R. T., Collins, R. J., and Candler, G. V., "Flight Measurements of Low Velocity Bow Shock Ultraviolet Radiation," *Journal of Thermophysics and Heat Transfer*, Vol. 7, No. 1, 1993, pp. 37–41.

[2]Levin, D. A., Candler, G. V., Collins, R. J., Erdman, P. W., Zipf, E. C., Espy, P. J., and Howlett, C. L., "Comparison of Theory with Experiment for the Bow Shock Ultraviolet Rocket Flight," *Journal of Thermophysics and Heat Transfer*, Vol. 7, No. 1, 1993, pp. 30–36.

[3]Candler, G. V., Levin, D. A., Collins, R. J., Erdman, P. W., Zipf, E. C., and Howlett, C. L., "Theory with Plume Radiance Measurements from the Bow Shock Ultraviolet 2 Rocket Flight," *Journal of Thermophysics and Heat Transfer*, Vol. 7, No. 4, 1993, pp. 709–716.

[4]Soule, H. V., *Electro-Optical Photography at Low Illumination Levels*, Wiley, New York, 1968.

[5]McGregor, W. K., Drakes, J. A., Beale, K. S., and Sherrell, F. G., "The AlCl Absorption Feature in Solid Rocket Plume Radiation," AIAA Paper 92-2917, July 1992.